$Ni\alpha_{SH}$ in Figure 4.) The heme pocket of the $Ni\alpha_{SH}$-subunits is known to be more spacious,[30-32] allowing the nickel porphyrin in more active sites to ruffle. The ruffled conformers would be expected to have lower affinity for axial ligands because of their smaller equatorial Ni-N bond distance. Thus, in the more spacious heme pocket of the isolated α-subunits, less histidine is bound, even though when histidine is bound (five-coordinate sites) the Ni-histidine force constant is greater for $Ni\alpha_{SH}$ than for NiHbA.[24,25] Apparently, by forcing the macrocycle into a planar conformation, the protein can increase ligand affinity. This suggests a possible mechanism for protein control of axial ligand affinity for nickel tetrapyrrole containing enzymes like methylreductase.

For derivatives of cofactor F_{430}, a nickel tetrapyrrole cofactor of the methylreductase enzyme, it is thought that axial ligation at the nickel(II) ion is controlled by the degree of planarity of the hydrocorphin macrocycle.[2-4,33] The great out-of-plane flexibility of this highly reduced porphyrin macrocycle suggests two possible mechanisms by which the protein might participate in the methyl-transfer reaction catalyzed by methylreductase. Because the size of the central core is determined by the macrocycle planarity, the protein can control the core size by varying planarity. In turn, by varying the core size, the protein forces can modify the ligand binding properties. Moreover, protein control over ruffling (and therefore core size) could be important for the redox function of methylreductase, since the Ni ion cycles between the large Ni(I) ion and small Ni(II) ion during the catalytic cycle.[34,35] Finally, protein control of macrocycle conformation may explain the large differences between the anomalous Raman spectrum of methylreductase and the spectra of the isolated F_{430} complexes.[4,33]

The crystal structure of native hemoglobin shows a domed macrocycle.[5] Therefore, the presence of a nonplanar conformation suggests a strained linkage through the proximal histidine that counters the strong forces holding the macrocycle into a planar conformation. The energy associated with the strain is stored not only in the Fe-histidine bond and its connection to the subunit interfaces but also the contacts with the pocket residues that oppose the nonplanar conformation.

In summary, the ruffling of nickel porphyrins in solution is shown to be a general effect for a variety of biologically significant porphyrin macrocycles. Environmental perturbations, such as π-π complex formation and dimerization, have a marked effect on the planarity of the macrocycle. Further, binding of nickel porphyrins to heme proteins has an even larger effect on macrocycle conformation and also a possible influence on chemical properties such as axial ligand affinity. It is clear from the present work that reconstitution of nickel porphyrins into heme proteins provides a new method of investigating nonbonding contacts in the active sites of proteins and of determining the importance of macrocycle distortions in the biological function of enzymes. It is also apparent from this study that the structural flexibility of the macrocycle might play an important role in understanding hemoprotein dynamics. This is especially true when the metal tetrapyrrole group experiences conformational distortions associated with biological function.

(33) Shiemke, A. K.; Shelnutt, J. A.; Scott, R. A. *J. Biol. Chem.* **1989**, *264*, 11236.
(34) Albracht, S. P. J.; Ankel-Fuchs, D.; Böcher, R.; Ellermann, J.; Moll, J.; van der Zwann, J. W.; Thauer, R. K. *Biochim. Biophys. Acta* **1988**, *955*, 86.
(35) Stolzenberg, A. M.; Stershic, M. T. *J. Am. Chem. Soc.* **1988**, *110*, 6391.

Structure and Basicity of Silyl Ethers: A Crystallographic and ab Initio Inquiry into the Nature of Silicon-Oxygen Interactions

Soroosh Shambayati,[†] James F. Blake,[‡] Scott G. Wierschke,[‡] William L. Jorgensen,*[,‡] and Stuart L. Schreiber*[,†]

Contribution from the Department of Chemistry, Harvard University, Cambridge, Massachusetts 02138, and Department of Chemistry, Purdue University, West Lafayette, Indiana 47907. *Received May 6, 1989*

Abstract: Analyses of the Cambridge Structural Database and results of ab initio molecular orbital calculations provide insights into the bond angle widening at oxygen and lowered basicity observed for silyl ethers in comparison to alkyl ethers. Common rationalizations for the phenomena based on interactions of oxygen lone pairs with silicon 3d orbitals and on steric effects do not find support. However, an alternative explanation that considers the detailed nature of the highest occupied molecular orbitals and concepts from Walsh diagrams accounts for the structural and chemical observations in a comprehensive manner.

The novel structural and chemical properties of silyl ethers are closely related. A striking geometrical observation is the widening of the bond angle about oxygen along the series, dimethyl ether ($\angle$C-O-C = 112°),[1] methoxysilane ($\angle$Si-O-C = 121°),[2] and disiloxane ($\angle$Si-O-Si = 144°).[3] This effect has been addressed in a variety of theoretical studies applying ab initio molecular orbital methods during the last ten years.[4-12] Attribution of the trend to mixing of oxygen lone-pair (n) and silicon 3d orbitals[2,3,13,14] has been challenged[4-7,11,12] though not entirely abandoned.[8] The dissenters have proposed enhanced steric effects and electrostatic

[†] Harvard University.
[‡] Purdue University.

(1) Blukis, V.; Kasai, P. H.; Meyers, R. J. *J. Chem. Phys.* **1963**, *38*, 2753.
(2) (a) Glidewell, C.; Rankin, D. W. H.; Robiette, A. G.; Sheldrick, G. M.; Beagly, B.; Freeman, J. M. *J. Mol. Struct.* **1970**, *5*, 417. (b) Blake, A. J.; Ebsworth, E. A. V.; Henderson, S. G. D.; Dyrbusch, M. *Acta Crystallogr.* **1988**, *C44*, 1 (CSD refcod: FUTZEZ).
(3) Almenningen, A.; Bastiansen, O.; Hedberg, K.; Traetteberg, M. *Acta Chem. Scand.* **1963**, *17*, 2455.
(4) Sauer, J.; Zurawski, B. *Chem. Phys. Lett.* **1979**, *65*, 587.
(5) Oberhammer, H.; Boggs, J. E. *J. Am. Chem. Soc.* **1980**, *102*, 7241.

0002-7863/90/1512-697$02.50/0

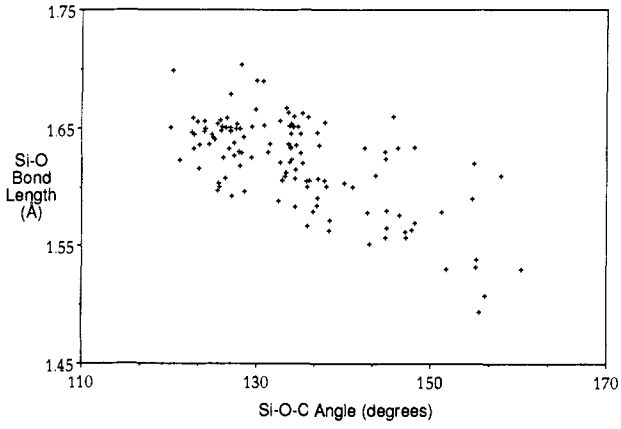

Figure 1. Correlation of Si–O bond lengths and Si–O–C bond angles for acyclic Si–O–C fragments with four-coordinated silicon. Data for Figures 1–3 from the Cambridge Structural Database (CSD).

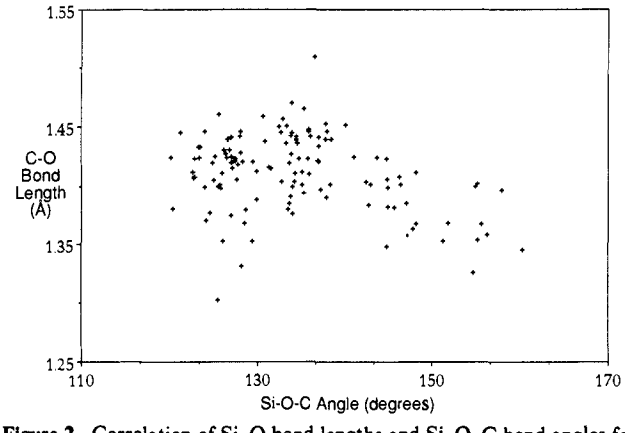

Figure 2. Correlation of Si–O bond lengths and Si–O–C bond angles for $(CH_3)_3Si$–O–C fragments.

repulsion for silyl groups compared to methyl.[4-6,11,12] Nevertheless, delocalization of the nonbonding orbitals on oxygen into empty orbitals on silicon could also nicely account for the low oxygen basicity of silyl ethers and the apparent absence of chelation in β-siloxy carbonyl/Lewis acid complexes.[14-16] In light of the importance of the silyl ether function in organic chemistry, particularly as a protecting group in synthesis, further investigations of the geometrical and electronic structures of silyl ethers are warranted. Through the present combined analysis of crystallographic data and results of ab initio calculations, a comprehensive explanation emerges for the geometrical preferences and chemical characteristics of silyl ethers. Neither steric effects nor n → 3d delocalization need to be invoked; instead, simple realizations from orbital interaction diagrams and a close look

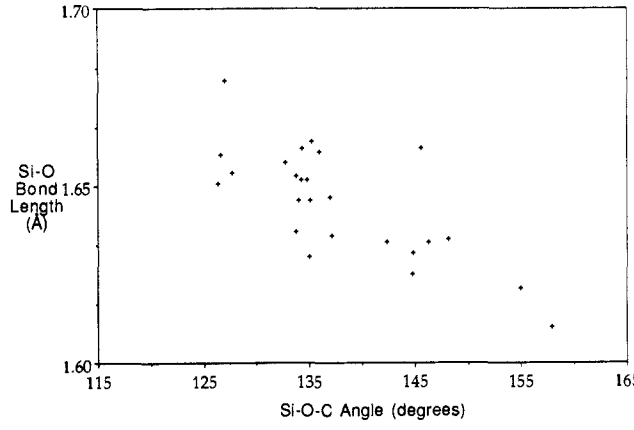

Figure 3. Correlation of C–O bond lengths and Si–O–C bond angles for the Si–O–C fragments of Figure 1.

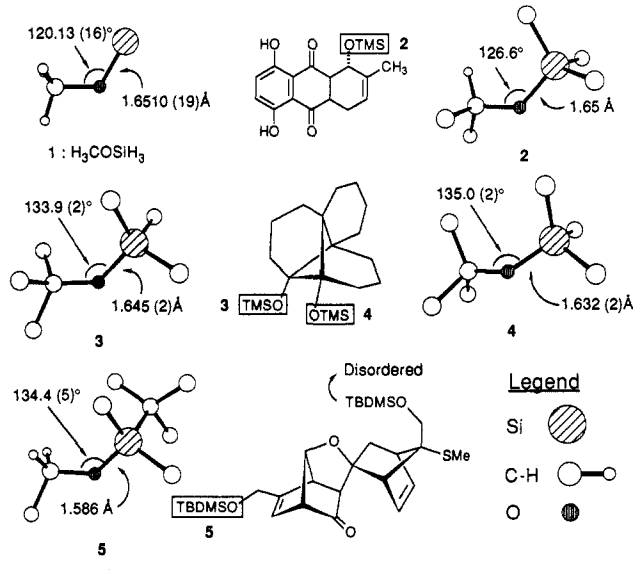

Figure 4. Comparison of Si–O–C bond angles and Si–O bond lengths from various crystal structures (ref 2b, 20, 21, and 24).

at highest occupied molecular orbitals reveal fundamental changes upon replacement of an alkyl group by a silyl group.

Statistical Analysis of Crystallographic Data

A principal motivation for analyzing crystal structures was to address the proposed importance of steric effects in the angle widening.[6,11,12] If the angle about the oxygen atom is opened by steric repulsion between the substituents, the bonds to the substituents should concomitantly lengthen. This correlation is routinely observed in conformational equilibria.[17] For example, ab initio calculations (MP2/6-31G[d]) find that in passing from anti to syn butane the C(2)–C(3) bond lengthens from 1.525 to 1.555 Å, while the C–C–C angle widens from 112.9 to 116.4°.[17a]

A connectivity search of the Cambridge Structural Database (CSD) for acyclic Si–O–C_{sp3} fragments with four-coordinated silicon revealed 127 such substructures with an average Si–O–C bond angle of 134.2° and Si–O bond length of 1.62 Å.[18] As shown in Figure 1, the clear trend is for the Si–O bond length to decrease with increasing Si–O–C bond angle; a linear least-squares fit yields

(6) Ernst, C. A.; Allred, A. L.; Ratner, M. A.; Newton, M. D.; Gibbs, G. V.; Moskowitz, J. W.; Topiol, S. *Chem. Phys. Lett.* **1981**, *81*, 424.
(7) Luke, B. T.; Pople, J. A.; Krogh-Jesperson, M. B.; Apeloig, Y.; Chandrasekhar, J.; Schleyer, P. v. R. *J. Am. Chem. Soc.* **1986**, *108*, 260.
(8) Kahn, S. D.; Keck, G. E.; Hehre, W. J. *Tetrahedron Lett.* **1987**, *28*, 279.
(9) Gibbs, G. V.; D'Arco, P.; Boisen, M. B., Jr. *J. Phys. Chem.* **1987**, *91*, 5347.
(10) Ignat'ev, I. S.; Shchegolev, B. F. *Dokl. Akad. Nauk.* **1987**, *296*, 143.
(11) Grigoras, S.; Lane, T. H. *J. Comput. Chem.* **1987**, *8*, 84.
(12) Grigoras, S.; Lane, T. H. *J. Comput. Chem.* **1986**, *9*, 25.
(13) Almenningen, A.; Hedberg, K.; Seip, R. *Acta Chem. Scand.* **1963**, *17*, 2264.
(14) (a) Varma, R.; MacDiarmid, A. G.; Miller, G. *Inorg. Chem.* **1964**, *3*, 1754. (b) Sternbach, B.; MacDiarmid, A. G. *J. Am. Chem. Soc.* **1961**, *83*, 3384.
(15) (a) Keck, G. E.; Castellino, S. *Tetrahedron Lett.* **1987**, *28*, 281. (b) Keck, G. E.; Boden, E. P. *Tetrahedron Lett.* **1984**, *25*, 265. (c) West, R.; Wilson, L. S.; Powell, D. L. *J. Organomet. Chem.* **1979**, *178*, 5. (d) Pitt, C. G.; Bursey, M. M.; Chatfield, D. A. *J. Chem. Soc., Perkin Trans. 2* **1976**, 434.
(16) Sauer, J. *Z. Chem.* **1982**, *22*, 60.

(17) For recent examples, see: (a) Wiberg, K. B.; Murcko, M. A. *J. Am. Chem. Soc.* **1988**, *110*, 8029. (b) Wiberg, K. B.; Schreiber, S. L. *J. Org. Chem.* **1988**, *53*, 783. (c) Wiberg, K. B.; Laidig, K. E. *J. Am. Chem. Soc.* **1987**, *109*, 5935.
(18) The original search of the CSD for *all* Si–O–C fragments (including cyclic and five-coordinated silicon atoms) produced 338 hits and a correlation coefficient of −0.541 between the Si–O bond length and the Si–O–C bond angle. Omission of the data for the special cases of five-coordinated and cyclic silicon fragments led to the better correlation factor discussed in the text. We are grateful to one of the referees for bringing this point to our attention.

Table I. Comparison of 6-31G(d) and Experimental Structural Parameters[a]

	r(C–O)		r(Si–O)		∠X–O–Y	
molecule	calc.	exptl	calc.	exptl	calc.	exptl
H_3COCH_3	1.391	1.410			113.8	111.7
H_3COSiH_3	1.400	1.418	1.640	1.640	125.0	120.6
H_3SiSiH_3			1.626	1.634	170.1	144.1

[a] Bond lengths in Å; bond angles in deg. Experimental data from ref 1–3.

a correlation coefficient of −0.68.[19] The correlation coefficient is −0.65 if the fit is restricted to the 25 trimethylsilyl substructures, $(CH_3)_3Si–O–C$, as illustrated in Figure 2. The results for the C–O bond length versus the Si–O–C angle for all 127 fragments show little correlation (Figure 3, correlation factor −0.32); the bond length certainly does not increase uniformly as the angle widens.

Inspection of individual crystal structures further highlights the inverse bond length/bond angle relationship. For example, trimethylsilyl ethers of primary, secondary, and tertiary alcohols exhibit progressively larger Si–O–C angles and shorter Si–O bonds with increasing steric congestion (cf. **1**, **2**, **3**, and **4** in Figure 4).[20-22] In extreme cases like **3** and **4**, some widening of the Si–O–C angle by steric effects is reasonable; however, it is accompanied by shortened Si–O bonds. Thus, a mechanism for the bond shortening is still needed such as the n → 3d mixing which would increase with more linear geometries or enhanced Si^+O^- polarity in the bonds which increases as the substituents on silicon are better able to stabilize the partial positive charge. The greater polarity would lead to greater electrostatic repulsion between the groups on oxygen,[5,6] and it could promote rehybridization at oxygen to use more s-character in the bonds to silicon.[7] This would, in turn, yield a wider angle and shorter Si–O bond. However, the polarity argument is inconsistent with the observed order of basicities,[14-16] $H_3COCH_3 > H_3COSiH_3 > H_3SiOSiH_3$, which was not considered in the earlier theoretical studies.[5,6]

It should be emphasized that the crystallographically observed correlations in Figures 1 and 2 are, by no means, perfectly linear and may be attenuated by a multitude of detailed geometrical, crystallographic, and electronic factors.[23] For example, although the *tert*-butyldimethylsilyl ether of a primary alcohol (**5** in Figure 4) and the trimethylsilyl ether of a tertiary alcohol (**3**) have very similar Si–O–C angles (134.4° and 133.9°, respectively), the Si–O bond of the latter is 0.06 Å longer.[24] Nevertheless, the general integrity of the inverse bond length/bond angle correlation for silyl ethers is apparent. It can also be found in related systems such as tri-*tert*-butoxysilicon groups. A striking illustration is provided within the crystal structure of **6**.[25] The Si–O–C angles are all relatively large in this structure and exhibit the inverse correlation. Thus, the Si(1)–O(1)–C(1) bond angle of 155.2° is considerably greater than the mean value for the Si–O–C angle

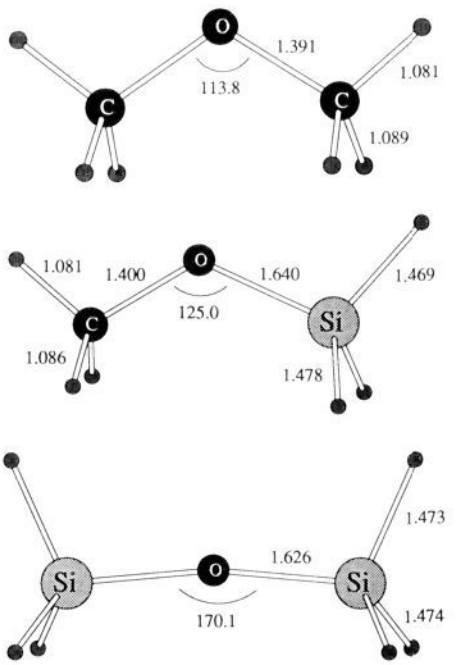

Figure 5. Optimized structures for dimethyl ether (top), methoxysilane (middle), and disiloxane (bottom) from 6-31G(d) calculations. Some key geometrical parameters are given with bond lengths in Å and bond angles in deg.

(134°), and the Si(1)–O(1) bond length (1.53 Å) is correspondingly shorter than the average Si–O bond length (1.62 Å). In comparison, the Si(2)–O(2)–C(2) fragment from the same molecule has a longer Si–O bond (1.61 Å) and a smaller Si–O–C angle (137.7°).

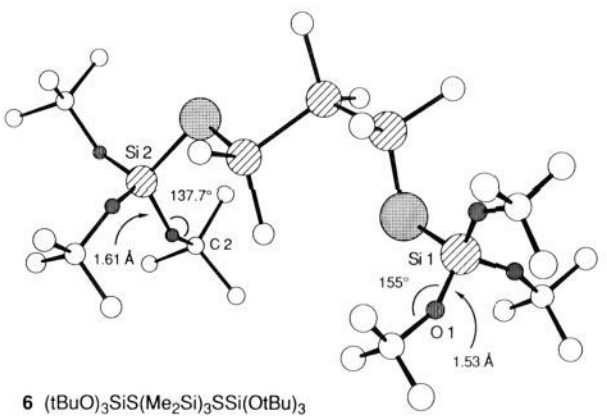

6 $(tBuO)_3SiS(Me_2Si)_3SSi(OtBu)_3$

Ab Initio Calculations

Restricted Hartree–Fock calculations were executed for $H_3C–OCH_3$, H_3SiOCH_3, $H_3SiOSiH_3$, $H_3SiOC(CH_3)_3$, $(CH_3)_3SiOCH_3$, and $(CH_3)_3SiOC(CH_3)_3$. The GAUSSIAN 82 program was used with the 3-21G and 6-31G(d) basis sets.[26] Both basis sets are of the split-valence type, and the latter includes a set of d-orbitals on each non-hydrogen atom. Complete geometry optimizations were carried out for the five smallest molecules with both basis sets using gradient methods, while the optimization for $(CH_3)_3SiOC(CH_3)_3$ was only performed at the 3-21G level. Additional computations were undertaken as described in the following.

H_3COCH_3, H_3SiOCH_3, and $H_3SiOSiH_3$. The calculations for this series of molecules were aimed at exploring the bond length/bond angle correlation and the origin of the angle widening at oxygen. Some key structural parameters from the 6-31G(d)

(19) According to simple statistical calculations, with a correlation coefficient of −0.68 in 127 pairs of observations there exists a 1% probability of no relationship between the two variables. The coefficient of determination is 46%. For example, see: (a) Olds, E. G. *Annals Math. Statistics* **1938**, 9. (b) McClave, J. T.; Dietrich, F. H. II *Statistics*; Dellen: San Francisco, CA, 1979; pp 423–425.

(20) Krohn, K.; Tolkiehn, K.; Lehne, V.; Schmalle, H. W.; Grützmacher, H.-F. *Liebigs Ann. Chem.* **1985**, 1311–1328 (CSD refcod: DIGHAC).

(21) Alder, R. W.; Arrowsmith, R. J.; Bryce, M. R.; Eastment, P.; Orpen, A. G. *J. Chem. Soc., Perkin Trans. 2* **1983**, 1519–1523 (CSD refcod: CAFBOA).

(22) In order to insure that the structures selected for inspection were representative of a particular class of structures, the data for each class was analyzed separately. The structures discussed here represent data points that were close to the best line of Si–O–C, Si–O correlation.

(23) In the absence of a systematic study of the structures of closely related silyl ethers, it is not possible to assess the exact Si–O, Si–O–C correlation. Thus the observed trend should be regarded as a qualitative rather than a quantitative relationship.

(24) Paquette, L. A.; Romine, J.; Barth, W.; Hus, L.-Y. *Tetrahedron Lett.* **1985**, *26*, 567–570 (CSD refcod: DABTOP).

(25) Wojnowski, W.; Dreczewski, B.; Peters, E.-M.; von Schnering, H. G. *Z. Anorg. Allg. Chem.* **1986**, *540*, 271–275 (CSD refcod: FIGJOU).

(26) Binkley, J. S.; Whiteside, R. A.; Raghavachari, K.; Seeger, R.; DeFrees, D. J.; Schlegel, H. B.; Firsch, M. J.; Pople, J. A.; Kahn, L. R. GAUSSIAN 82 *Release H*; Carnegie Mellon University: Pittsburgh, PA, 1982.

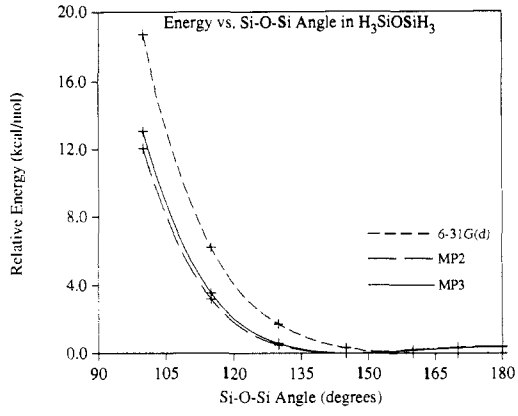

Figure 6. Calculated potential energy versus Si–O–Si angle in disiloxane.

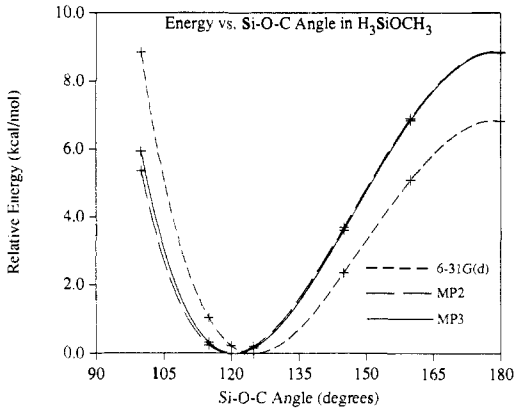

Figure 7. Calculated potential energy versus Si–O–C angle in methoxysilane.

optimizations are illustrated in Figure 5, and comparisons of the calculated and experimental C–O and Si–O bond lengths and central bond angles are given in Table I. The accord between theory and experiment for dimethyl ether and methoxysilane is excellent; however, the 6-31G(d) result for the Si–O–Si angle in disiloxane (170°) is substantially greater than the experimental gas-phase (144.1°)[3] and crystallographic (142.2°)[27] values.

Disiloxane is well-known to have an unusually flat Si–O–Si angle bending potential. The frequency for the motion appears to be 68 cm^{-1} from infrared studies,[28] and the inversion barrier has been established as 0.32 kcal/mol from a Raman investigation.[29] Under the circumstances, it seemed appropriate to test the influence of including electron correlation on the computed results. Geometry optimizations were carried out for seven fixed values of the Si–O–Si angle between 100° and 180° with the 6-31G(d) basis set. Single point calculations for the energies were then executed including correlation estimates from second- and third-order Møller–Plesset theory (MP3/MP2/6-31G[d]//6-31G[d]) excluding the core orbitals. This level of treatment is comparable to configuration interaction with full double excitations for the noncore MO's.[30] The results are illustrated in Figure 6. Indeed, the minimum is moved to 145° when the correlation energy is included. Furthermore, the predicted inversion barriers of 0.41 (MP2) and 0.38 kcal/mol (MP3/MP2) are in remarkable agreement with the experimental value.[29]

The influence of the correlation energy was tested in the same way for the Si–O–C angle bending in methoxysilane (Figure 7).

(27) Barrow, M. J.; Ebsworth, E. A. V.; Harding, M. H. *Acta Crystallogr. B* **1979**, *35*, 2093.
(28) (a) McKean, D. C. *Spectrochim. Acta* **1970**, *26A*, 1833. (b) Robinson, D. W.; Lafferty, W. J.; Aronson, J. R.; Durig, J. R.; Lord, R. C. *J. Chem. Phys.* **1961**, *35*, 2245.
(29) Durig, J. R.; Flanagan, M. J.; Kalasinsky, V. F. *J. Chem. Phys.* **1977**, *66*, 2775.
(30) Hehre, W. J.; Radom, L.; Schleyer, P. v. R.; Pople, J. A. *Ab Initio Molecular Orbital Theory*; Wiley: New York, 1986.

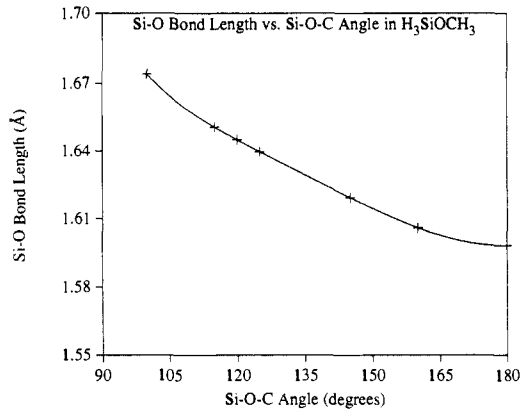

Figure 8. Si–O bond length versus Si–O–C angle in methoxysilane from the 6-31G(d) optimizations.

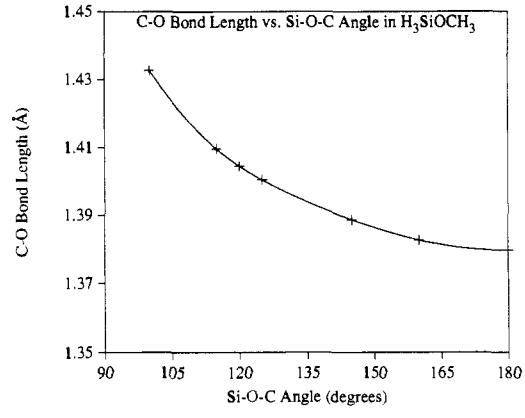

Figure 9. C–O bond length versus Si–O–C angle in methoxysilane from the 6-31G(d) optimizations.

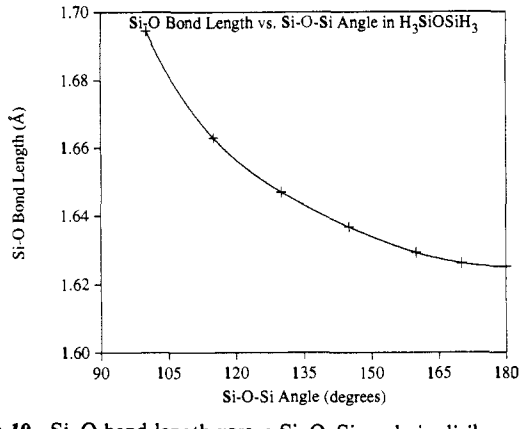

Figure 10. Si–O bond length versus Si–O–Si angle in disiloxane from the 6-31G(d) optimizations.

Though the minimum only shifts 5° from 125° at the 6-31G(d) level to 120° including the MP3/MP2 corrections, this does remove the discrepancy with the experimental result in Table I. The predicted inversion barriers for this molecule, 6.8 and 8.8 kcal/mol at the 6-31G(d) and MP3/MP2/6-31G(d) levels, are still notably low. For comparison, the inversion of dimethyl ether requires 36.3 kcal/mol according to our 6-31G(d) calculations.

The bond length/bond angle correlations were also studied with the 6-31G(d) optimizations for methoxysilane and disiloxane, as reported in Figures 8–10. Consistent with the crystallographic results in Figures 1 and 2, the Si–O bond lengths are found to decrease smoothly with increasing bond angle about the oxygen (Figures 8 and 10). The same trend is also revealed for the C–O bond length in methoxysilane (Figure 9), though the range is diminished for this intrinsically shorter bond.

Orbital Interactions, Angle Bending, and Basicity. These calculations provided a basis for deeper analysis of the correspond-

Chart I

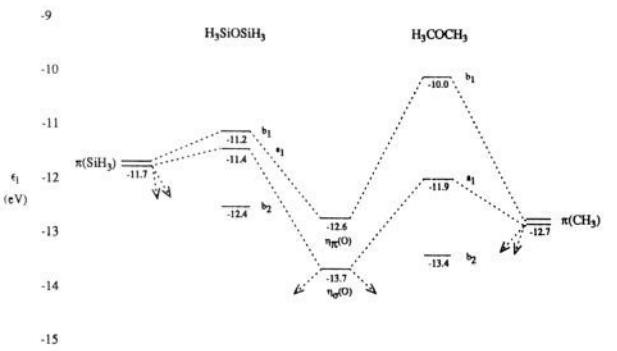

ences between electronic structure, geometry, and reactivity. First, if one is concerned about basicity, a careful look at highest occupied molecular orbitals (HOMO's) is essential. The following interaction diagram can be constructed for the highest occupied MO's of bent dimethyl ether and disiloxane from experimental data on ionization potentials.[31-33] The key interactions are between the π and σ type lone-pair orbitals on oxygen and the degenerate $\pi(CH_3)$ and $\pi(SiH_3)$ group orbitals for the substituents.[34] The π orbitals for the two XH_3 groups combine to form in-phase and out-of-phase combinations; only the former have the right symmetry to interact with n_π and n_σ. The reference energies for the $\pi(XH_3)$ orbitals can be taken from the ionization potentials of methane (12.7 eV) and silane (11.7 eV), while the reference

energies for n_π and n_σ can be assigned from the two lowest ionization potentials of water (12.6 and 13.7 eV).[32] The three lowest ionization potentials for dimethyl ether and disiloxane are also known[33] and allow completion of the illustrated interaction diagram.

Plots of the HOMO and HOMO-1 for the two molecules in Figure 11 can now shed light on the origins of the significantly higher ionization potential of disiloxane (11.2 eV) as compared to that of dimethyl ether (10.0 eV). The plots were constructed with the PSI/88 program[35] from the 6-31G(d) wave functions at contour levels of ±0.1 au. For dimethyl ether, the HOMO is the expected out-of-phase combination of the n_π and $\pi(CH_3)$ orbitals mixed in a comparably weighted fashion. The HOMO-1 for dimethyl ether is the out-of-phase mixture of n_σ with the other $\pi(CH_3)$ combination. This orbital does reveal hybridization at oxygen with noticeable bulging in the lone-pair direction. Significant differences are apparent in the corresponding MO's for disiloxane. As expected, the contributions on oxygen are much diminished, and, in fact, the orbitals are primarily localized on the hydrogens. There is no clear evidence for the involvement of d-orbitals on silicon; indeed, the largest coefficient for a silicon d-orbital is only 0.07 in the 6-31G(d) HOMO which translates to less than 1% of the electron density in the orbital. This is consistent with prior ab initio results and with the observation that the d-orbitals are not needed to obtain the central angle widening upon silyl substitution.[4-6,11] The latter result was also confirmed by the present 3-21G calculations (vide infra).

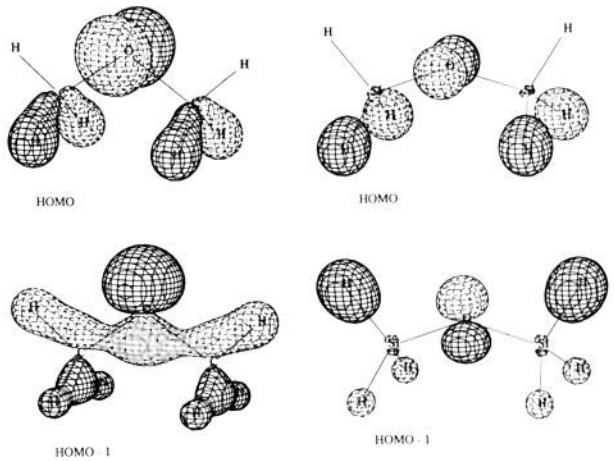

Figure 11. The HOMO and HOMO-1 for dimethyl ether (left) and disiloxane (right) from the 6-31G(d) wave functions at a contour level of ±0.1 au.

More surprisingly, there is little evidence of the p-orbital on silicon in both MO's as compared to the clear p contributions on carbon. The origin of this observation can be rationalized based on the mixing of the HOMO and HOMO-1 with the $\pi^*(XH_3)$ orbitals in a constructive fashion. Due to the lower energy of

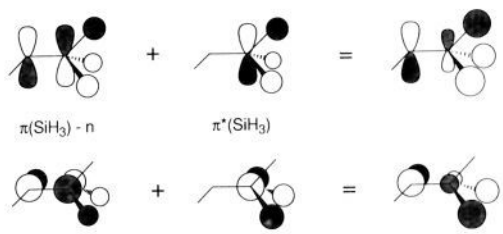

$\pi^*(SiH_3)$ (relative to $\pi^*(CH_3)$) this effect is expected to be greater when X = Si. The outcome is a small p component on silicon and reinforcement of the coefficients on hydrogen, just as in Figure 11.[36]

The interactions with the $\pi^*(SiH_3)$ orbitals are a form of delocalization of the lone-pair orbitals on oxygen into unoccupied orbitals on silicon, and they favor a linear geometry at oxygen. They also contribute to a more fundamental reason for the relative resistance to deviations from linearity for the Si–O–C and Si–O–Si angles.

The bending of AX_2 molecules is promoted by mixing of an oxygen 2p orbital (HOMO) in the linear form with the σ^* LUMO.[31] For disiloxane, the HOMO has significantly diminished 2p character on oxygen compared to dimethyl ether, because of both the relatively higher energies of the $\pi(SiH_3)$ orbitals and lower energies of the $\pi^*(SiH_3)$ orbitals. Consequently, the overlap with the LUMO on bending is reduced, and the energetic gain from rehybridization is lessened. Confirmation of this effect is provided by the present ab initio results; the decline in the energy of the HOMO-1 upon bending from linearity occurs at about half the rate for disiloxane as for dimethyl ether. In addition, the lack of hybridization at oxygen in the HOMO-1 for disiloxane is apparent in Figure 11. Thus, for disiloxane, the lowering of the HOMO-1 upon bending is less capable of compensating for the raising of the b_2 MO, which favors a linear geometry. This is the basic reason for the widening of the bond angle at oxygen upon substitution of silyl for methyl groups. Furthermore, the explanation for the inverse bond length/bond angle correlations (Figures 1, 2, 8, 9, and 10) is also straightforward; the b_2 orbital is stabilized

(31) For a thorough discussion, see: Albright, T. A.; Burdett, J. K.; Whangbo, M. H. *Orbital Interactions in Chemistry*; Wiley: New York, 1985; pp 93–97.
(32) Rosenstock, H. M.; Draxl, K.; Steiner, B. W.; Herron, J. T. *J. Phys. Chem. Ref. Data* **1977**, *6*, Suppl. 1.
(33) Bock, H.; Mollere, P.; Becker, G.; Fritz, G. *J. Organomet. Chem.* **1973**, *61*, 113.
(34) Jorgensen, W. L.; Salem, L. S. *The Organic Chemists Book of Orbitals*; Academic Press: New York, 1973.
(35) Jorgensen, W. L.; Severance, D. L. Unpublished extended version of PSI/77. Jorgensen, W. L. *QCPE* **1980**, *12*, program 340.
(36) An analogous three-way orbital interaction has been regularly invoked in discussions of hyperconjugation.[34] For other examples, see: (a) Hoffmann, R.; Radom, L.; Pople, J. A.; Schleyer, P. v. R.; Hehre, W. J.; Salem, L. *J. Am. Chem. Soc.* **1972**, *94*, 6222. (b) Wierschke, S. G.; Chandrasekhar, J.; Jorgensen, W. L. *J. Am. Chem. Soc.* **1985**, *107*, 1496.

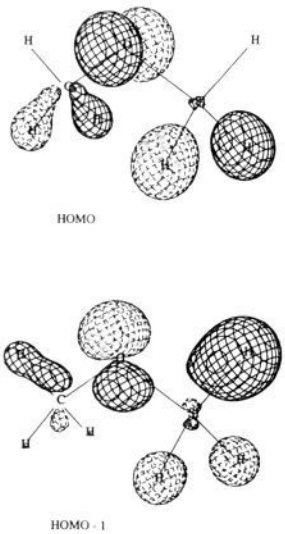

Figure 12. The HOMO and HOMO-1 for methoxysilane from the 6-31G(d) wave function at a contour level of ±0.1 au.

at wider angles which provides better overlap along the Si–O and C–O bonds and bond strengthening.

Methoxysilane represents an intermediate case between disiloxane and dimethyl ether. The experimental ionization potentials for the HOMO and HOMO-1 are 10.6 and 11.5 eV[33] and may be assigned to the orbitals in Figure 12.[37] Greater contributions from the $\pi(SiH_3)$ and $\pi^*(SiH_3)$ group orbitals than from the methyl group orbitals are apparent and lead to the diminished oxygen lone-pair character relative to the MO's for dimethyl ether (Figure 11).

In view of the above analysis, the origin of the basicity order, $R_3COCR_3 > R_3SiOCR_3 > R_3SiOSiR_3$, is also readily understandable.[14-16] The oxygen basicity decreases upon replacement of alkyl groups by silyl groups because the energy of the HOMO declines and the HOMO becomes less localized on oxygen (Figures 11 and 12). Consequently, the key interaction between the ether HOMO and the LUMO of an electrophile is less stabilizing for silyl than for alkyl ethers.

$H_3SiOC(CH_3)$, $(CH_3)_3SiOCH_3$, and $(CH_3)_3SiOC(CH_3)_3$. The optimized 3-21G structures for these molecules are illustrated in Figure 13, and the 6-31G(d) structures for the two smaller molecules are in Figure 14. In each case, C_s symmetry was assumed. 3-21G and 6-31G(d) optimizations were also carried out for the alternate conformers of *tert*-butyl silyl ether (BSE) and methyl trimethylsilyl ether (MTMSE) with the *tert*-butyl and TMS groups rotated 60°. In all instances the illustrated conformers were 0.4–1.1 kcal/mol lower in energy. For *tert*-butyl trimethylsilyl ether (BTMSE), the 3-21G calculations were only performed for the conformation with the end groups rotated as in the preferred forms for the smaller molecules.

The Si–O–C angles in Figure 13 are widened from the 3-21G results of 130.4° for methoxysilane. Not surprisingly, the widest angle, 144.8°, is computed for BTMSE. Interestingly, these structures do show the inverse bond length/bond angle correlation for the tertiary groups; the C–O and Si–O distances in BSE and MTMSE are 1.441 and 1.678 Å, respectively, while the corresponding bond lengths in BTMSE are 1.435 and 1.670 Å. The 3-21G and 6-31G(d) structures for the two smaller ethers are very similar (Figures 13 and 14) with the largest difference in bond lengths of only 0.035 Å. The Si–O–C angles for MTMSE and BSE increase by 2° and 9° from the value for methoxysilane (Figure 5) according to the 6-31G(d) calculations. Comparison of Figures 5 and 14 also reveals that the O–SiH_3 and O–CH_3 bonds shorten a little in going from methoxysilane to BSE and MTMSE. Another subtle effect in all of the computed structures is the longer C–X and Si–X bonds to the out-of-plane substituents than the in-plane ones. This can be largely attributed to the expected greater mixing of the n_π than the n_σ orbital with the $\pi^*(CR_3)$ and $\pi^*(SiR_3)$ group orbitals. The mixing and the bond length differentiation sould be greater for the silyl substituents, as observed.

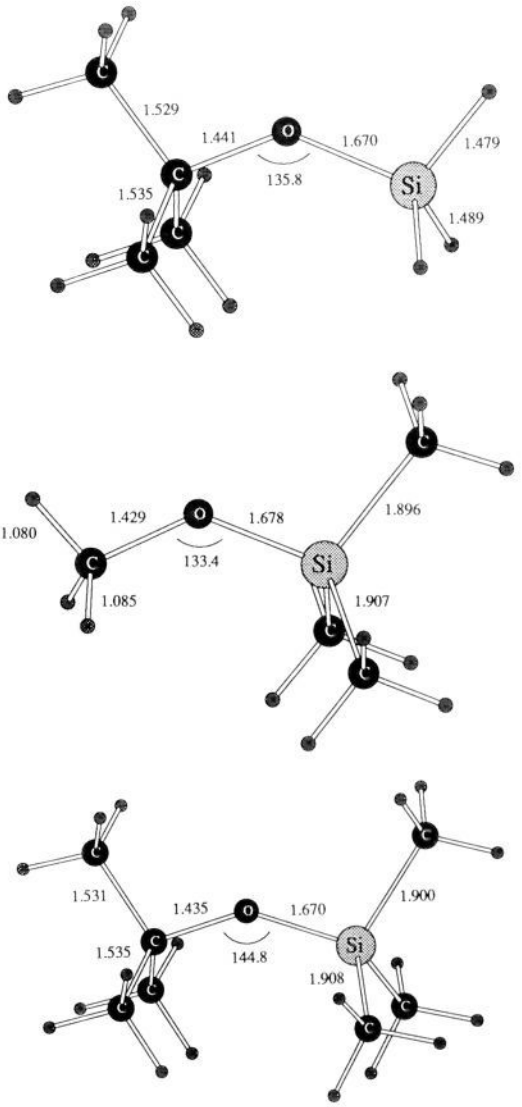

Figure 13. Optimized structures for BSE (top), MTMSE (middle), and BTMSE (bottom) from 3-21G calculations.

The origin of the Si–O–C angle widening upon increasing the size of the substituents on oxygen probably has a steric component. However, as discussed above, this would not explain the shortening of the Si–O and C–O bonds. An alternative MO-based argument would contribute these observations to the higher initial energies for the $\pi(Si(CH_3)_3)$ orbitals (vs $\pi(SiH_3)$)[32] and the greater mixing of the n orbitals with the $\pi^*(Si(CH_3)_3)$. Thus, the HOMO's for the more substituted silyl ethers would be expected to be even more concentrated on the silyl groups. This is verified by the MO plots for the HOMO and HOMO-1 of MTMSE in Figure 15. These orbitals have only secondary oxygen lone-pair character; they

(37) The orbital assignments in the photoelectron study were based on CNDO/2 calculations.[33] The present ab initio results concur on the assignment of the b_1 HOMO and a_1 HOMO-1 for dimethyl ether and methoxysilane. However, the original assignment[33] of the HOMO-1 as the b_2 orbital for disiloxane is incorrect on the basis of the present findings; it is still the a_1 orbital as shown in Figure 11.

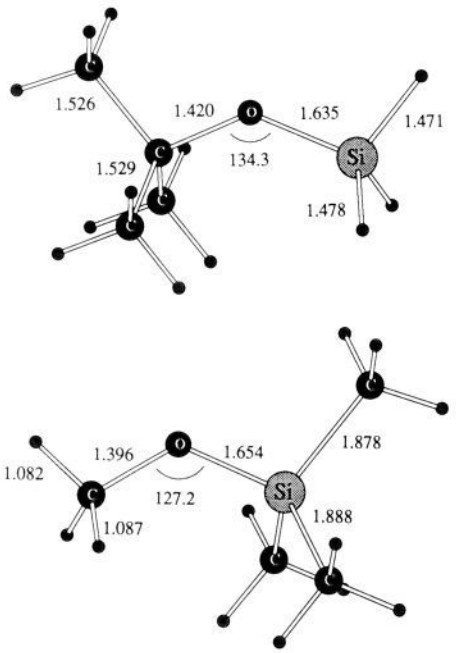

Figure 14. Optimized structures for BSE (top) and MTMSE (bottom) from 6-31G(d) calculations.

primarily reflect the TMS group orbitals. The implications are that the HOMO–LUMO mixing on bending and rehybridization of the oxygen are even less effective at stabilizing the n_σ orbital than for methoxysilane, so the Si–O–C angle widens and a shorter Si–O bond length is observed.

Conclusions

The present analyses of crystal structures and ab initio MO calculations rule out the common notions that steric effects or n → d interactions are primarily responsible for the wide Si–O–C bond angles and low oxygen basicity of silyl ethers. Statistical analyses of X-ray crystallographic data clearly indicate trends which counter predictions based only on steric arguments. A frontier orbital analysis of the problem shows that these observations follow from two factors: (a) the higher energy of $\pi(SiR_3)$ than $\pi(CR_3)$ group orbitals and the poorer mixing of the $\pi(SiR_3)$ orbitals with the oxygen lone pairs due to the required 2p-3p overlap and (b) some mixing of the lone-pair orbitals with the relatively low-lying $\pi^*(SiR_3)$ group orbitals. Both effects lead to lower energies and smaller oxygen components for the HOMO's of silyl ethers compared to alkyl ethers and to wider bond angles at oxygen.

The interpretation of the crystallographic data also benefits from the theoretical results in the context of the observed reactivity patterns of silyl ethers. For example, consider the observation of the enhanced stability of silyl ethers toward acid hydrolysis upon an increase in the steric bulk of the silicon substituents. Crystallographic data show that larger silicon substituents result in a widening of the Si–O–C angle and shorter Si–O bond lengths. Superficially, this observation may seem to suggest lower oxygen

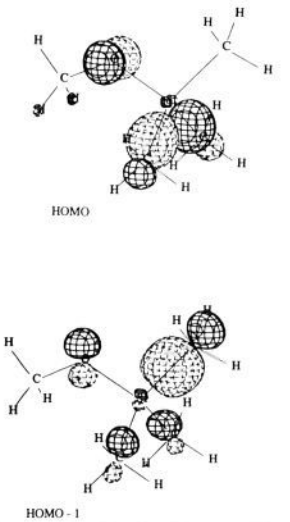

Figure 15. The HOMO and HOMO-1 for MTMSE from the 6-31G(d) wave function at a contour level of ±0.1 au.

basicity for larger silyl ethers due to increased Si–O interaction; however, theory suggests otherwise. Although widening of the Si–O–C angle would cause the oxygen components in the HOMO's to be reduced, the HOMO's will also be of higher energy at wider angles, and the larger molecules are more polarizable. The latter factor will likely dominate in determining the basicities, as measured by proton or hydrogen bonding affinities, that should increase for silyl ethers with increasing bulk, just as for alkyl ethers.[15c,39] Therefore, we suggest that, in contrast to its value for the prediction of basicities in going from alkyl ethers to silyl ethers to disiloxanes, the angle about the oxygen atom cannot be used to predict relative basicities within each class. For example, while this angle can be correlated to the differences in the oxygen basicities of a benzyl- versus a trimethylsilyl ether, the correlation between the Si–O–C angle and the oxygen basicities may be completely different (even reversed) in comparing trimethylsilyl and *tert*-butyldimethylsilyl ethers. The relative hydrolysis rates may be simply controlled by steric hindrance to solvent assistance for the Si–O bond cleavage following the protonation step. This and other interesting issues about the structure and chemistry of silyl ethers should continue to provide opportunities for refinement of both synthetic methods and theoretical models.[40]

Acknowledgment. Gratitude is expressed to Kurtis MacFerrin for his invaluable assistance with the implementation of the CSD on a VAXstation 3500 computer and to Dr. Neville Anthony for insightful comments. Support for this research by a grant from the NIGMS (to S.L.S.) and grants from the NSF (to S.L.S. and W.L.J.) is gratefully acknowledged.

(38) Colvin, E. *Silicon in Organic Synthesis*; Butterworths: London, 1981; pp 178–192.
(39) Lias, S. G.; Liebman, J. F.; Levin, R. D. *J. Phys. Chem. Ref. Data* **1984**, *13*, 695.
(40) Shambayati, S.; Schreiber, S. L. In *Comprehensive Organic Synthesis*; Trost, B. M., Ed.; Pergamon Press: London, in press.